Heavy Mesons Produced by 2.2- and 3.0-Bev Protons*

R. D. HILL,† E. O. SALANT, AND M. WIDGOFF‡
Brookhaven National Laboratory, Upton, New York
(Received March 24, 1955)

Emulsions were traversed by radiations from a target bombarded by either 2.2-Bev or 3.0-Bev protons. Analyses of tracks of twelve heavy mesons that came to rest in the emulsions are presented. The stopped heavy mesons produced secondaries showing that 2 were tau mesons, 1 was a negative K meson, and 9 were positive K mesons. Grain count, scattering and range measurements served to determine K-meson masses; the average of 6 positive K mesons that could be measured well was $(965\pm15)m_e$. Evidence is given, from comparison with existing $p\beta$-blob density curves, that one K^+ secondary is a muon or electron, while another K^+ secondary is a pion. If, in the latter case, it is assumed that the K^+ decays into a charged and a neutral pion, the mass of the K^+ is found to be $(945\pm20)m_e$ and the Q of the decay (207 ± 9) Mev, the same, within experimental error, as for θ^0.

INTRODUCTION

DURING the past year and a half, the heavy mesons θ^0, τ, K^-, and K^+ have all been produced, either by 2.2- or 3-Bev protons, or by 1.5-Bev pions, at the Cosmotron.[1–4]

Although data on heavy mesons have been accumulating rapidly in cosmic-ray observations,[5] such data do not often include knowledge of the nature and energy of the producing particle. Such knowledge is available in accelerator experiments, which have the further advantage that a known, localized target can be used, and emulsions can be so placed that radiations from the target traverse them in planes approximately parallel to their surfaces. This arrangement makes for easier scanning and longer K-meson tracks than does the arrangement in which the emulsion itself is the target.

The target was in the straight section of the Cosmotron, and the path of its radiations to the detecting emulsions was entirely in this field-free region. Magnetic analysis of the radiations from the target has also been done, but this paper reports only those experiments in which the K mesons were not magnetically selected.

EXPERIMENTAL ARRANGEMENTS

Stacks of 24 strips of 2 in.×3 in. 400μ Ilford G5 nuclear emulsions were exposed at either of two positions outside the Cosmotron vacuum chamber, as illustrated in Fig. 1(a), or inside the vacuum chamber, adjacent to a target, mounted as shown in Fig. 1(b). For each exposure, the target, held on a plunging ram, was kept in a position shielded from the proton beam for most of the Cosmotron's accelerating cycle. At the end of each cycle, the target was plunged into a position such that it was struck only by protons of full energy. Exposures were limited by the number of background tracks which arose from: (i) pions and protons coming directly from the target, (ii) stars produced in the emulsion and surrounding material by secondaries from the target. It was found that satisfactory scanning with a 20× dry objective could be carried out on emulsions which had a flux of the order of 10^4 minimum ionizing track per cm^2.

For the emulsion stacks exposed as shown in Fig. 1(a), particles entering the emulsions from the target penetrated the 0.47-inch thick steel wall of the Cosmotron. This served to reduce the intensity of evaporation particles from disintegrations in the target, and to slow

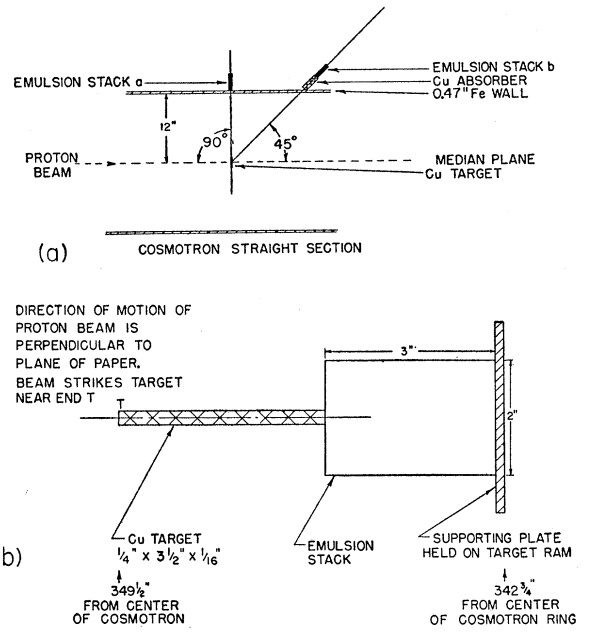

FIG. 1. Experimental arrangement. Figure 1(a) shows the positions of emulsions *LT*2, *LT*3 and *LT*5, relative to the target and the proton beam of the Cosmotron. Figure 1(b) shows the method of mounting emulsions *LT*7 and *LT*11, for exposures inside the vacuum chamber of the Cosmotron.

* Work performed under the auspices of the U. S. Atomic Energy Commission.
† Now at the University of Illinois, Urbana, Illinois.
‡ Now at Harvard University, Cambridge, Massachusetts.
[1] Fowler, Shutt, Thorndike, and Whittemore, Phys. Rev. **93**, 861 (1954).
[2] J. Hornbostel and E. O. Saland, Phys. Rev. **93**, 902 (1954).
[3] Hill, Salant, and Widgoff, Phys. Rev. **94**, 1794 (1954); **95**, 1699 (1954).
[4] Hill, Salant, Widgoff, Osborne, Pevsner, Ritson, Crussard, and Walker, Phys. Rev. **94**, 797 (1954).
[5] C. F. Powell, Nuovo cimento **11**, Suppl. 2, 165 (1954).

TABLE I. Summary of exposures.

Exposure code number	Exposure details	Number of protons in circulating beam (approximate)	Flux of lightly ionizing particles	Number of K particles observed
LT 3*a*	2.2 Bev Fig. 1(a) 90°	0.8×10^9	2×10^4/cm²	0
LT 2*b*	2.2 Bev Fig. 1(a) 45°	0.7×10^9	5×10^3/cm²	1
LT 5*a*	3.0 Bev Fig. 1(a) 90°	1.2×10^9	3×10^3/cm²	8
LT 5*b*	3.0 Bev Fig. 1(a) 45°	1.9×10^9	4×10^3/cm²	1
LT 7	3.0 Bev Fig. 1(b) 90°	4.7×10^9	5×10^4/cm²	2
LT 11	2.2 Bev Fig. 1(b) 90°	8.8×10^9	5×10^4/cm²	0

down the K particles. Several exposures, e.g., those at 45° to the proton beam, were made with additional absorbers between the target and the emulsions. These absorbers were used to reduce the energies of the K particles emitted in the forward direction so that some would come to rest in the emulsion stack. The stacks exposed inside the vacuum chamber were shielded from the target by $\frac{5}{32}$ in. of Cu; however, evaporation tracks made the plates difficult to scan in the area adjacent to the target.

Table I gives a summary of the exposures. The energies of the incident protons, the numbers of the figures which illustrate the geometry of the exposures, and the angles between proton beam and the detected secondaries are given in column 2. In column 3 are given the total numbers of protons in the circulating beam during the exposures, and in column 4 are given the fluxes of lightly ionizing particles traversing the emulsions. The numbers of K particles, including τ mesons, observed in the emulsions, are given in column 5.

DETAILS OF SCANNING AND OBSERVATIONS

The emulsions were area-scanned under a 20× objective for tracks of particles reaching the end of their range. In this way σ stars, π-μ decays, μ-e decays, K-particle interactions and decays, and proton track endings were observed. The emulsions were clear and the average minimum grain count was high (~38 grains/100μ), so that the presence or absence of a light outgoing track could be determined easily. Where there was any doubt, the ending was checked under high magnification (90× objective).

In Table II are given the results of this systematic scanning. Column 2 gives the area scanned for each stack. Columns 3–6 give the numbers of light-meson endings. Column 4 includes both one-prong σ stars, and those π-μ events in which the μ did not decay in the stack. Column 8 gives the number of K mesons found in the area listed in column 2. Columns 7 and 9 give, for π mesons and K particles, respectively, the approximate limits within which the particle energies must lie when they leave the target, in order for them to come to rest in the part of the emulsion which was scanned. These limits were calculated with the assumption that the particles traversed the absorber between target and emulsion in a straight line, and entered the emulsion through the edge of the stack.

In addition to the K particles listed in Table II, several were found in random scanning of some areas of the plates: two ($K7$ and $K9$) in $LT5a$ and two, including one τ meson, in $LT7$. No systematic scanning has yet been done on the $LT7$ and $LT11$ stacks.

A check was made of the direction of entry of the π mesons that stopped in the emulsions, and it was found that more than three-fourths came from the direction of the target.

In Table III are given some of the details of the K-particle tracks observed. Columns 2–4 give, respectively, the total track length in the emulsion stack, the average track length per emulsion strip, and the maximum track length in a single strip. Column 5 shows whether the particle entered through the edge of the stack, in which case the particle could have come directly from the target, or through one of the 2-inch ×3-inch surfaces of the stack, in which case the K particle must have undergone scattering, or must have been produced in surrounding material by secondaries. The tracks of all the K particles which entered the stack through the edge facing the target lay within the angular spread of the beam from the target. Column 6 gives the energy of the particle on entering the emulsion. For the particles coming from the target direction, the energies on leaving the target have been calculated on the assumption that they traveled straight through the intervening absorber. These values are given in column 7.

Of the K particles listed here, $K1$ made a small star at the end of its range, and was thus identified as a K^- particle; $\tau1$ and $\tau2$ were identified as such because at the end of their range they underwent the characteristic decay into three coplanar charge light mesons; the remaining mesons $K2$ to $K10$ each came to rest in the emulsion and gave rise to a lightly ionizing particle, with no other visible secondary, and are phenomenologically identified as K^+ particles which have decayed.

We believe that the scarcity of K^- stars relative to K^+ endings is not due to scanning inefficiency. About $\frac{3}{4}$ of K^- stars have, in addition to 1 or more black prongs, a fast particle.[6] Our efficiency for finding and identifying such stars is appreciably higher than for finding K^+ endings, hence the ratio of K^+ mesons to star-forming K^- mesons should be even higher than the present observations indicate.

[6] J. Hornbostel and E. O. Salant, Phys. Rev. 98, 218 (1955).

TABLE II. Results of systematic area scanning.

Exposure code number	Area scanned (cm^2)	Number of light meson track endings: σ stars, 2 or more prongs	Number of light meson track endings: 1-prong σ stars and π-μ events	Number of light meson track endings: π-μ-e	Number of light meson track endings: μ-e	Observable π-meson energy interval (Mev)	Number of K particles found in systematic scanning	Observable K-particle energy interval (Mev) (approximate)
LT 3*a* (2.2 Bev, 90°)	15.0	105	317	133	173	70–100	0	120–150
LT 2*b* (2.2 Bev, 45°)	62.0	192	551	213	357	160–195	1	260–300
LT 5*a* (3.0 Bev, 90°)	53.4	255	775	250	504	45–90	6	80–145
LT 5*b* (3.0 Bev, 45°)	27.3	38	114	34	98	160–195	1	260–300

Any comparison of rates of K-particle production at different energies and different angles that can be made from the data given in Tables I and II is uncertain, partly because of the small number of K particles observed, and partly because of uncertainties in the relative intensities of the different exposures. Neither the number of stopping pions and muons, nor the flux of lightly ionizing particles, assumed to consist mostly of light mesons, can be used as a measure of exposure intensity, since the cross section for production of these mesons is not known as a function of angle and primary energy. The circulating-beam monitor cannot be used reliably in a quantitative way at the low intensities used for the exposures, although it was used as a guide in timing them. Thus, there is no basis for a quantitative comparison of yields at different energies. There is no evidence for an appreciable change in the yield at 45° in going from a primary energy of 2.2 Bev to 3.0 Bev; at 90°, although many more K mesons were found at 3.0 Bev than at 2.2 Bev, it should be noted that the observable energies were higher and the energy interval was narrower at 2.2 Bev.

The same uncertainty in relative intensities does not apply to comparison of the numbers N of K mesons observed at 45° and 90°, with incident 3.0-Bev protons. The exposures at the two angles were for the most part simultaneous; the 45° plates were exposed somewhat longer to compensate, to some extent, for the smaller solid angle subtended. After correction for solid angle, relative exposure as measured by the circulating beam monitor, and area scanned, the ratio is $N(90°)/N(45°) = 1.8_{-1.2}{}^{+0.4}$. The error is the statistical standard deviation. The loss by decay is not significantly different at the two positions, if a lifetime equal to the lower limit 5×10^{-9} sec given by Astbury *et al.*[7] is assumed.

The expected value of this ratio has been calculated by Sternheimer,[8] by assuming that K mesons are produced in reactions of the type p+nucleon→Λ^0+K+nucleon, with target nucleons having energies that follow a Gaussian distribution with an average energy of 20 Mev. Two possible angular distributions of the K particles in the center-of-mass system have been considered: one is isotropic, and the other varies as $\cos^2\theta$. For each of these, two possible distributions in energy have been assumed: one, f_1, is proportional to the relativistic phase space factor times a constant matrix element; the other, f_2, is proportional to the phase space factor times $p_K{}^2$, where p_K is the momentum of the K particle in the center-of-mass system. Of these, only the isotropic distribution, with the energy distribution f_1, seems inconsistent with the measured ratio.

MASSES OF K PARTICLES

One of the most important questions associated with K particles is whether the particles with different charges and decay properties have the same or different masses.

The most accurately determined K-particle masses are those of the θ^0 and τ mesons which have masses of $(966\pm10)m_e$ and $(965.5\pm0.7)m_e$, respectively.[9,10] Although, individually, the measured masses of most K particles are distributed widely throughout the range from $\sim800m_e$ to $\sim1300m_e$, there appears to be general acceptance[11] that the K-particle mass probably lies at approximately $1000m_e$. In particular, the group of workers[12] at l'Ecole Polytechnique have reported a value of $(913\pm20)m_e$ for the mass of S particles found in their cosmic-ray experiments with cloud chambers. However, in spite of the improvement in statistics and techniques of mass measurements, there are still in the literature some outstanding cases of K particles with masses significantly higher than $\sim1000m_e$. The first K particle observed at Bristol was reported to

[7] Astbury, Buchanan, Chippindale, Millar, Newth, Page, Rytz, and Sahiar, Phil. Mag. **44**, 242 (1953).

[8] R. S. Sternheimer, Phys. Rev. **93**, 642 (1954), Brookhaven Internal Reports RS-41, RS-42, RS-44, RS-46 (unpublished) and private communication.

[9] Thompson, Burwell, Cohn, Huggett, and Karzmark, Phys. Rev. **95**, 661(A) (1954).

[10] Amaldi, Fabri, Hoang, Lock, Scarsi, Touschek, and Vitale, Nuovo cimento **12**, Suppl. 2 (Padua Conference), 419 (1954).

[11] C. F. Powell, Report of Bagnères Conference, p. 222 (1953); Nuovo cimento **11**, Suppl. 2, 165 (1954).

[12] Gregory, Lagarrigue, Leprince-Ringuet, Muller and Peyrou, Nuovo cimento **11**, 292 (1954); L. Leprince-Ringuet, Proceedings of the Fourth Annual Rochester Conference (University of Rochester Press, Rochester, 1954).

TABLE III. Details of K-particle tracks.

K particle and stack in which it was found	Total track length in stack (mm)	Average track length per emulsion strip (mm)	Max. length in a single strip (mm)	Surface at which particle entered stack	Energy of particle when it entered emulsion (Mev)	Approximate energy of particle when it left target (Mev)
$K1$ *LT 2b*	31.5	6.5	11.3	edge facing target	78	275
$K2$ *LT 5a*	45.1	3.8	9.3	edge facing target	96	125
$K3$ *LT 5a*	21.3	3.0	9.1	edge facing target	62	100
$K4$ *LT 5a*	42.5	2.8	9.1	edge facing target	93	120
$K5$ *LT 5b*	10.4	0.95	1.5	edge facing target	42	260
$K6$ *LT 5a*	13.5	2.7	4.0	edge facing target	48	90
$K7$ *LT 5a*	9.4	3.1	3.7	2 in.×3 in. surface	38	...
$K8$ *LT 5a*	21.8	3.6	6.8	edge facing target	62	100
$K9$ *LT 5a*	18.2	2.6	4.2	2 in.×3 in. surface	57	...
$K10$ *LT 7*	4.1	4.1	4.1	2 in.×3 in. surface	24	...
$\tau 1$ *LT 5a*	33.9	17.0	17.5	edge facing target	82	115
$\tau 2$ *LT 7*	1.2	1.2	1.2	2 in.×3 in. surface	12	...

have a mass of approximately $1300m_e$,[13] and another of 1300–$1400m_e$ was reported[14] at Paris. There are also, apart from the observed stopping K particles, the jet-produced K particles, discovered by Daniel and Perkins[15] and reinvestigated by Fowler and Perkins,[5] which have a mass of approximately $1450m_e$.

Because the tracks of the K mesons we observed were generally more than 1 cm long, the particle mass was usually most conveniently and precisely determined by grain density-range measurements. In several cases, masses were also determined by the method of scattering-range.

(1) Masses Determined by the Method of Grain Density Range

Owing to the comparatively heavy development of our emulsions, which had a minimum grain count of $\sim$38 grains per 100μ, the average grain density of K-particle tracks at 12 mm residual range was approximately 100 grains per 100μ, and at 24 mm approximately 80 per 100μ. No grain counts were made at residual ranges less than 1 cm because of the high grain density.

Of the twelve K particles tabulated in Table III, eight gave tracks from which masses were measured by the method of grain density range. The tracks were grain-counted in those emulsions for which a reasonably long segment of track existed and for which the residual range was as large as possible. In the same emulsions, under the same conditions of counting and as nearly as possible at the same time, measurements of grain density range were made on π mesons, and, in a few cases, μ mesons, with which the measurements of the K particles were compared. Pions and muons were used for calibration because our emulsions contained large numbers of them, and in general they could be found satisfactorily close ($\sim$1 cm or less) to the region in which the K mesons were being counted. In each case, in order to be certain that the calibration particles had not decayed or interacted in flight, it was required that at least one of the calibrating tracks be that of a π^+ meson which decayed into a muon of approximately 600μ range, the standard range of muons from pions which have come to rest. Usually only those calibrating tracks that were sufficiently long in one emulsion (the one being studied) were accepted. The calibrating tracks were grain-counted over an interval of grain density that included the K-particle grain density in the plate. In order to reduce the possibility of systematic errors, each K-particle mass was determined against at least two calibrating tracks in a given emulsion strip, and, whenever possible, similar measurements were made in more than one strip of the stack.

When the grain densities of the K particle and its calibrating tracks had been determined, a plot was made, for each type of particle (K, π, or μ meson), of y, the logarithm of grain density per mm of tracks, *vs* x, the logarithm of the residual range R, and a least

[13] C. O'Ceallaigh, Phil. Mag. **42**, 1032 (1951); S. von Friesen, Proceedings of the Bagnères Conference, 1953 (unpublished), p. 128; C. F. Powell, Nuovo cimento **11**, Suppl. 2, 165 (1954).

[14] L. Leprince-Ringuet, Proceedings of the Fourth Annual Rochester Conference (University of Rochester Press, Rochester, 1954), p. 72.

[15] R. Daniel and D. Perkins, Proc. Roy. Soc. (London) **A221**, 351 (1954).

squares line, $y=a+bx$, was fitted to each set of points. All of these lines should have the same slope, and, in fact, the fitted slopes were found to agree with each other within the statistical errors. The average, $\bar{b}$, of these slopes, weighted according to their statistical errors, was determined. A new line was then drawn for each type of particle, by passing a line of slope $\bar{b}$ through the center of gravity, $\bar{x}=\sum_i w_i x_i/\sum_i w_i$, $\bar{y}=\sum_i w_i y_i/\sum_i w_i$, of each set of points, where the w_i are the statistical weights of the individual points x_i, y_i. The K-particle mass was determined from the ratio of the ranges at equal grain density of the K track and calibration track. For example, if one takes $y=\bar{y}_\pi$ as the constant grain density line, then

$$\frac{M_K}{M_\pi}=\frac{R_0}{\bar{R}_\pi}=\frac{\exp x_0}{\exp \bar{x}_\pi}, \tag{1}$$

where

$$x_0=(\bar{y}_\pi-\bar{y}_K)/\bar{b}+\bar{x}_K, \tag{2}$$

and the statistical standard error is given by

$$\frac{\epsilon(R_0)}{R_0}=\left[\frac{1}{\bar{b}}\frac{(0.76)^2}{N_\pi}+\frac{1}{\bar{b}}\frac{(0.76)^2}{N_K}+\frac{(\bar{y}_\pi-\bar{y}_K)^2}{\bar{b}}\sigma^2(\bar{b})\right]^{\frac{1}{2}}. \tag{3}$$

Here N_π and N_K are the total counted numbers of π-meson and K-meson grains, respectively, and $\sigma^2(\bar{b})$ is the statistical error in the weighted average slope $\bar{b}$. Similarly, one can obtain M_K/M_μ.

Of course, the ratio obtained by taking the range intercepts with any line of constant grain density will be the same, but the error will be changed somewhat from that given above. It is necessary to limit the range and grain density interval over which one fits a straight line, as the slope of the ln$g$ *vs* ln$R$ line is not constant over large intervals. Usually, points representing a grain density variation of not more than 10 grains per 100μ were fitted by a single line. The slope is then rather poorly determined by the points, since the range interval covered is small. It is, therefore, desirable, in order to minimize the importance of the slope in determining the range intercepts, to choose calibration tracks such that their $\bar{y}$ will be as close as possible to $\bar{y}_K$.

The results of the mass determinations by the method of grain density-range are given in Table IV. The values given there were obtained by using $m_\pi=273.4m_e$ and $m_\mu=207.0m_e$.[16] Column 2 gives the range intervals and the emulsion strip numbers in which the mass determinations were made; column 4 gives the number and kind of calibrating tracks used; columns 3 and 5 give the total numbers of grains counted in K-particle and calibrating tracks, respectively. In column 6 are given the K-particle mass values determined separately for each emulsion strip, with the standard statistical errors found by means of Eq. (3). Column 7 gives the weighted average mass value and standard statistical error for each particle. In most of the cases where the same K particle was measured in two emulsions, the mass values are in agreement within the statistical errors; differences might be an indication of errors arising from nonstatistical sources such as irregularities in the emulsion.

The masses given in Table IV, including those of negative ($K1$), positive ($K2$, $K3$, $K4$, $K6$, $K8$, $K9$) and τ mesons, are in satisfactory agreement with one another, within limits of about $70m_e$. The value of the τ-meson mass is also in accord with the value of $965.5m_e$,[10] determined from the three-pion decay of the τ meson. The weighted average value of the K^+-particle mass, obtained from the K^+ masses given in Table IV, excluding $\tau 1$, is $(965\pm15)m_e$. The error given is the standard statistical error. It should be noted that the decay products of the K^+ mesons have not been identified in most cases, and that several different decay schemes are probably represented. Thus this average does not represent the mass of any particular species of K particle.

(2) Masses Determined by the Method of Scattering-Range

There are two approaches to the measurement of masses by the method of scattering-range: for long tracks, constant cell lengths can be used to measure the scattering at large residual range, while for short tracks, measurements can be made by using constant sagitta methods.[17]

The masses of several of the K particles have been measured by one or both of these means.

Tracks that were long and flat, in the emulsion strips where the residual ranges were large, were suitable for constant cell-length measurements. The track of $\tau 1$ satisfied the requirements very well, and since the mass of the τ meson is well known, the other K-particle masses were obtained by comparing the scattering measurements on them with those made on the τ-meson track, in the following way.

From 119 cells of 100μ length, the mean scattering angle for the τ meson in the residual range interval from 17.5 mm to 29.9 mm was measured to be $0.216°\pm0.013°$. This value was obtained from the mean second differences measured with 100μ and 200μ cells, by using the noise elimination technique of Menon, O'Ceallaigh, and Rochat.[18] The error is the statistical error determined by the number of independent 200μ cells, as defined by O'Ceallaigh and Rochat.[19] By using the known mass of the τ particle and the effective residual

[16] Smith, Birnbaum, and Barkas, Phys. Rev. **91**, 765 (1953).

[17] Biswas, George, and Peters, Proc. Indian Acad. Sci. **38**, 418 (1953); Dilworth, Goldsack, and Hirschberg, Nuovo cimento **11**, 113 (1954).

[18] Menon, O'Ceallaigh, and Rochat, Phil. Mag. **42**, 932 (1951).

[19] C. O'Ceallaigh and O. Rochat, Phil. Mag. **42**, 1050 (1951).

TABLE IV. K-particle masses determined by the method of grain density *vs* range.

K particle	Residual range interval (mm) and emulsion strip in which grain count was made	Total grains counted in K-particle track	Kind and number of calibrating tracks	Total grains counted in calibrating tracks	K-particle mass values (m_e)	Weighted average values of K-particle mass (m_e)
$K1$	15.2–19.9 (2*b*.15)	3733	4π 2μ	7577	970±55	980±30
	19.9–27.4 (2*b*.16)	5410	2π 1μ	8266	985±35	
$K2$	10.8–20.1 (5*a*.10)	8988	4π	15028	955±30	940±25
	20.1–23.9 (5*a*.11)	3079	4π	9168	910±40	
$K3$	12.0–21.0 (5*a*.16)	9253	3π	11630	1005±35	1005±35
$K4$	16.1–23.1 (5*a*.19)	5897	3π	11957	965±30	975±25
	23.1–32.2 (5*a*.20)	6788	3π	6266	1010±60	
$K6$	11.0–13.4 (5*a*.17)	2545	3π	9637	955±70	955±70
$K8$	14.3–19.3 (5*a*.23)	4641	3π	8624	950±40	975±40
	19.8–22.2 (5*a*.24)	2022	2π	4532	1305±145	
$K9$	13.8–16.3 (5*a*.23)	2344	3π	8624	950±45	950±45
$\tau 1$	10.0–16.6 (5*a*.11)	6611	2π	6723	970±65	955±25
	19.4–29.5 (5*a*.10)	8948	2π	8378	955±30	

range R, defined by Gottstein and Mulvey[20] as

$$R=\left[\frac{0.15(R_2-R_1)}{R_1^{-0.15}-R_2^{-0.15}}\right]^{0.87},$$

where R_2 and R_1 are the ranges at the beginning and end of the interval measured, a value of K_s, the scattering constant in the equation $p\beta=K_s/\bar{\alpha}_{100}$, may be obtained by trial and error, from the universal curves of $p\beta/R$ *vs* β and p/Mc *vs* β. From the above data, a value of K_s equal to (25.8±1.5) (Mev/c)-degree was thus derived. Although this value in no way represents an improved determination of the scattering constant, it is nevertheless a direct and independent check of the scattering method. The masses of $K1$, $K2$ and $K4$, on which scattering measurements could be made at approximately the same residual range as for $\tau 1$, have been determined by using the value of 25.8 (Mev/c)-degree for the scattering constant. The values of the masses, together with the range intervals in which the measurements were made, the effective residual ranges and the mean scattering angles, are given in Table V. In all cases, the mean scattering angles were determined as in the case of $\tau 1$,[18] and the errors in the mass values are those which arise from the statistical errors in $\bar{\alpha}_{100}$.[19]

Values of K-particle masses measured by constant sagitta methods, with the variable cell length schemes of Biswas, George, and Peters[17] and of Fay, Gottstein, and Hain[21] are given in Table VI.

The mass values determined by scattering with cells of constant length (Table V) are in agreement, within the errors, with those obtained from grain density measurements (Table IV). The mass values determined by constant-sagitta scattering methods (Table VI) do not seem to be consistent with the results of the other methods; except in the case of $K1$, they are considerably higher. We believe that the constant-sagitta methods are not reliable for the short track lengths we have used; the results have been found to be inconsistent from

[20] K. Gottstein and J. H. Mulvey, Phil. Mag. **42**, 1089 (1951).

[21] Fay, Gottstein, and Hain, Nuovo cimento **11**, Suppl. 2, 234 (1954).

one part of a track to another, and from one cell length scheme to another. It also seems possible that there is a systematic error, which could arise from a variation of the scattering constant with range, at small residual range.

The best mass determinations are those based on grain density measurements, which yield an average of $(965\pm15)m_e$. The determinations from scattering are of considerably lower statistical accuracy. Inclusion of the constant cell length scattering values with the grain density values does not change the average mass, and also does not improve the accuracy. Inclusion of the constant-sagitta results as well increases the average mass to $1000m_e$, again with no significant improvement in accuracy. Because of the inconsistencies of these constant-sagitta measurements, the final average mass, obtained by omitting them, is accordingly taken to be $(965\pm15)m_e$.

NATURE OF CAPTURE OR DECAY OF K PARTICLES

The manner in which K particles are captured or decay is of prime interest in the study of these particles. In the following sections, the capture of one K^- particle, the decays of two τ mesons and of four K^+ particles are analyzed.

(1) Capture of a K^- Meson

An illustration of the star produced by the capture of $K1$ is shown in Fig. 2. The center of the star shows considerable evidence of low-energy electron tracks, probably from Auger electrons associated with the capture of the K^- into the emulsion atom, although it cannot be certain that they are not merely background tracks. There is no evidence either for a recoil track of for a high-energy electron ($\gtrsim$50 kev). However, the last section of the K^- track is so dense that the existence of a short recoil track in the backward direction, obscured by the incoming track, could not be ruled out.

Of the two visible outgoing tracks, one has a low grain density and is 2.14 mm long in the first emulsion strip, 1.04 mm in the adjacent strip. The particle then produced in flight a star of two black tracks. The other outgoing particle from the K^- star was heavily ionizing and traveled a total of 969μ in three emulsion strips before coming to rest.

Scattering measurements were made on both the outgoing tracks from the K^- star. The heavily ionizing particle was found to have range and $p\beta$ corresponding to those of a proton emitted with an energy of (13.5 $\pm$0.5) Mev. The lightly ionizing particle had a $p\beta$ of (125$\pm$30) Mev/c which is consistent with either a pion of (75$\pm$25) Mev or a proton of (62$\pm$15) Mev.

Grain density measurements on the light track showed a small variation from 1.64 to 1.71 times minimum in passing along the track from the K^- star to the secondary star. These grain density measurements are consistent with a pion of (50$\pm$5) Mev or a proton of (300$\pm$20) Mev. We must conclude from the consistency of scattering and grain density data that the lightly ionizing particle was a pion of approximately 50 Mev.

TABLE V. K-particle masses determined by method of scattering *vs* range, with constant length cells of 100μ and 200μ and scattering constant of 25.8 (Mev/c)-degree.

K particle	Residual range interval (mm)	Effective residual range (mm)	Mean scattering angle $\bar{\alpha}_{100}$ (degrees)	Mass (m_e)
$\tau1$	17.5–29.9	23.2	0.216	965.5 (standard)
$K1$	19.8–27.2	23.2	0.216	970$\pm$240
$K2$	20.2–27.3	23.4	0.208	1040$\pm$270
$K4$	23.1–32.2	27.4	0.205	881$\pm$200

The angle between the outgoing pion and proton tracks was measured on a tilting stage microscope to be 135°$\pm$2°.

A point of particular interest in the analysis of K^- stars is their characteristically low energy.[22–24] In the present K^- star there is direct evidence of only 203 Mev of emitted energy (including the pion rest energy), whereas the energy available from complete conversion of the K^- particle is approximately 500 Mev.

Any scheme suggested to account for this star must predict the emission of a 50-Mev charged pion. It is not necessary to account specifically for the 13-Mev proton, which could result from evaporation. The products of K capture may include hyperons[6,25,26] (the hyperons Λ and Σ, of rest energy 1115 Mev and 1190 Mev, respectively, will be considered presently), but, since there is no such track in the star, any charged hyperon must be regarded as reabsorbed within the parent nucleus, a process discussed by Goldhaber.[26] Various schemes will now be discussed.

Consider, first, capture of a K^- meson by a single nucleon N at rest in a nucleus. Let the process be limited to the production of two particles and let these

TABLE VI. K-particle masses determined by the method of scattering *vs* range, with constant sagitta.

K particle	Residual range interval (mm)	Mass[a] (m_e)	Mass[b] (m_e)
$K1$	0–2.1	1090$\pm$300	800$\pm$180
	0–11.3	800$\pm$130	750$\pm$110
$K2$	0–3.6	1380$\pm$300	1450$\pm$290
$K3$	0–4.2	···	1430$\pm$260
$K7$	0–2.5	···	1540$\pm$340
$K10$	0–4.0	1320$\pm$290	1100$\pm$200

[a] See reference 17.
[b] See reference 21.

[22] Lal, Pal, and Peters, Proc. Indian Acad. Sci. **38**, 398 (1953).
[23] J. Hornbostel and E. O. Salant, Phys. Rev. **93**, 902 (1954).
[24] C. F. Powell, Nuovo cimento **11**, Suppl. 2, 165 (1954).
[25] H. DeStaebler, Jr., Phys. Rev. **95**, 1110 (1954).
[26] M. Goldhaber, Phys. Rev. **92**, 1279 (1953); see also R. H. Dalitz, Phys. Rev. **94**, 1046 (1954).

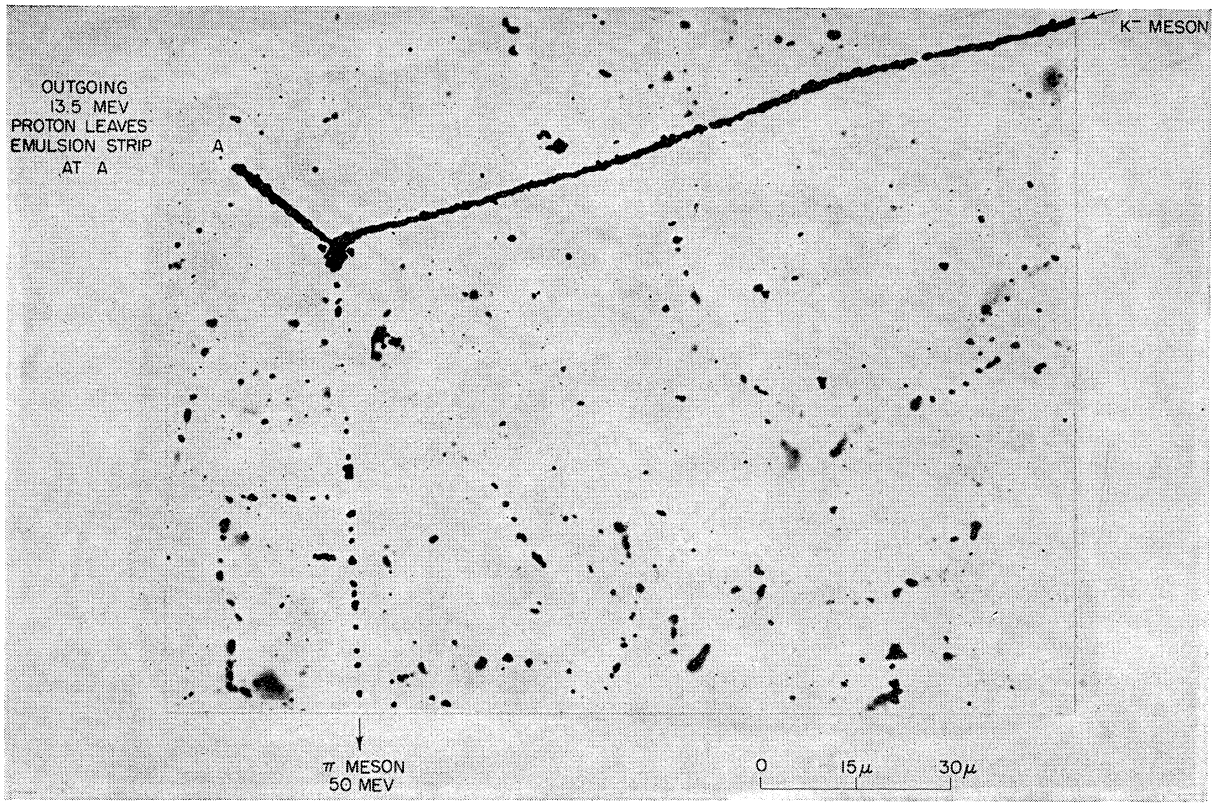

FIG. 2. Star produced by capture of K^- meson. A K^- meson coming from the right is shown stopping and producing a two-prong star of a π meson and a proton.

two particles emerge without interacting with any of the nucleons of the nucleus.

In the following reactions, where the Q values are in Mev,

$$K^-+N\rightarrow\pi^-+N+353, \quad (1)$$

$$K^-+N\rightarrow\pi^-+\Lambda^0+178, \quad (2)$$

$$K^-+N\rightarrow\pi^-+\Sigma^0+102, \quad (3)$$

the kinetic energies of the pions are 280 Mev for (1), 150 Mev for (2) and 87 Mev for (3), each inconsistent with the observed pion energy. It is to be noted that the K-meson rest energy is too low to produce a pion in addition to a cascade particle (rest energy $\sim$1315 Mev).

However, if the target nucleon is not at rest, then, as a consequence of Fermi energy, the pion of reaction (3) might be observed with 50 Mev, but not the pion of the first two reactions.

But even with a stationary nucleon, a 50-Mev pion can be obtained if any one of the other limitations is dropped. If the pion makes collisions with the other nucleons of the nucleus, it could lose enough energy. If the K-meson capture involves more than one nucleon, or produces more than two particles, as in

$$K^-+N+N\rightarrow\pi^-+N+N+353, \quad (1a)$$

$$K^-+N\rightarrow\pi^-+\pi^0+N+219, \quad (1b)$$

$$K^-+N+N\rightarrow\pi^-+\Lambda^0+N+178, \quad (2a)$$

momenta and energies can be balanced so as to accomplish the desired result.

An interesting alternative is the case discussed by Goldhaber,[26] where a hyperon (produced in K-meson capture) is trapped within the nucleus and subsequently emits a pion. Because its traversal time of a nucleus is much briefer than its lifetime, the hyperon must come to rest long before its break-up. But a Λ^0 decaying at rest yields only a 32-Mev pion; consequently a bound Λ^0 would not explain our K star. On the other hand, trapping of a Σ, produced in the reaction

$$K^-+N\rightarrow\pi^0+\Sigma^-+102 \quad (4)$$

would yield a 95-Mev charged pion, which, by collisions with nucleons, could emerge with 50 Mev. Similarly, a cascade particle, produced without an additional pion, could, if it decayed within the nucleus, yield a charged pion of the observed energy.

Thus it is apparent that many different schemes could

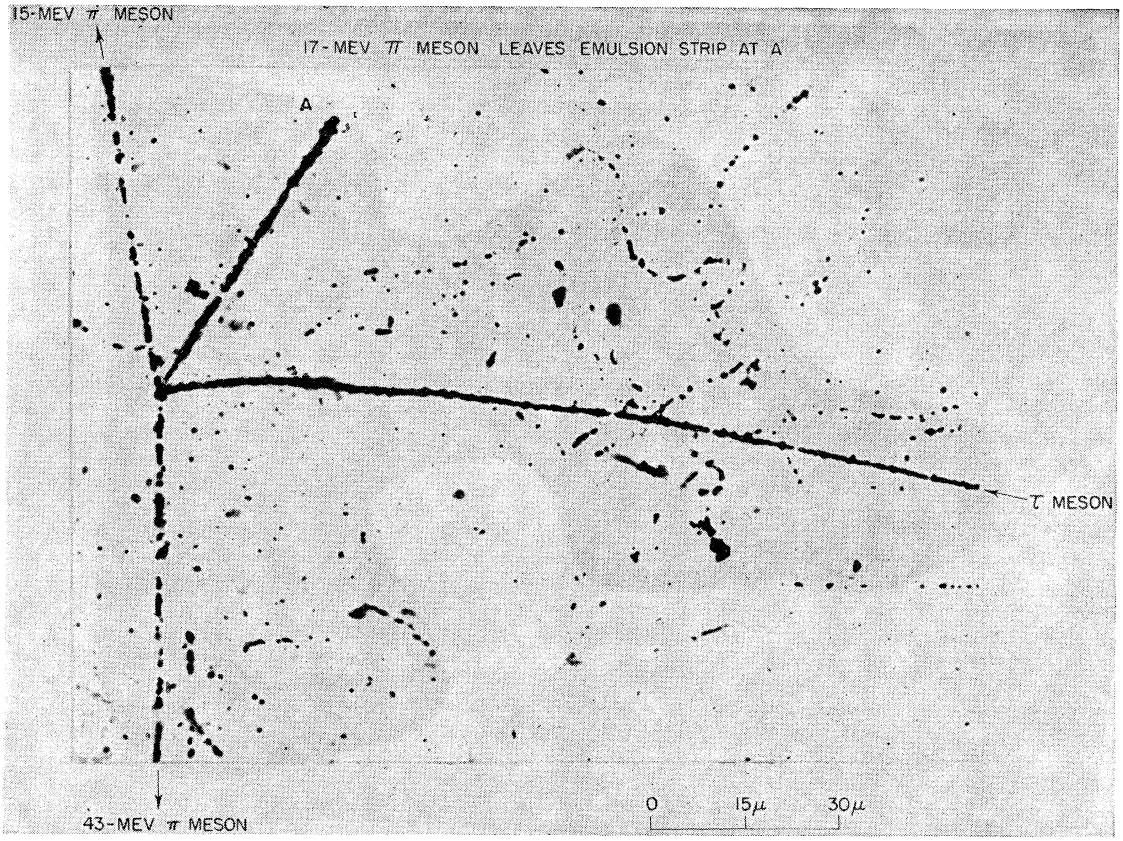

FIG. 3. Decay of τ meson. A τ meson coming from the right is shown decaying at rest into three coplanar charged π mesons.

account for our K^- star. Only reactions (1), (2) and (3) with all of the restrictions initially noted must be rejected, and (3) is acceptable with plausible Fermi energy.

So far, no account has been taken of the recent ideas of Pais and Gell-Mann and of Goldhaber, which restrict the possible products of K-meson capture.[26,27] Reactions (1), (1a), and (1b) are ruled out. In their schemes, any Σ particle in the presence of nuclear matter is transformed into a Λ^0, which then decays. Since, as we have seen, the decay of a Λ^0 will not yield a sufficiently energetic pion, neither will be Σ. Hence decay of the trapped Σ of reaction (4) will not do.

Consequently, if the theoretical restrictions are valid, the only mechanism that could yield the observed K star is the production of a charged pion and a hyperon, according to reactions (2a) or (3). The schemes of Pais and Gell-Mann and of Goldhaber forbid the formation of a cascade particle from K^- capture.

(2) Decay of τ Mesons

An illustration of the decay of $\tau 1$ is shown in Fig. 3. The details of the $\tau 1$-meson decay have already been given[3] and they are here merely summarized, together with those of $\tau 2$, in Table VII.

It is noteworthy that the ratio of the numbers of τ mesons and other K mesons, $\frac{1}{5}$, is the same as the ratio reported in cosmic rays.

(3) Decay of K^+ Mesons

A typical K^+ decay, $K2$, is shown in Fig. 4. Of the nine K^+ particles, five had secondary tracks which were too steep for reliable scattering measurements, as the track length per emulsion strip was 1 mm or less. Of the four secondary tracks considered suitable for measurement, $K2$ averaged 3.1 mm per strip; $K3$, 2.3 mm per strip; $K7$, 4.1 mm per strip; and $K10$ had a track length of 52.5 mm in a single strip. A preliminary report of $K10$ has been given.[28] None of the secondary tracks ended in the emulsion.

Grain and blob counts, as well as scattering measurements, were made on the four selected tracks. In order to obtain the ratio of the grain or blob density of a segment of track to the plateau grain or blob density, the plateau density in the neighborhood of each track segment was determined by blob- or grain-counting electrons from μ-e decays. The grain- and blob-count

[27] M. Gell-Mann and A. Pais, Proc. Glasgow Conference, July, 1954 (to be published); also private communication. M. Goldhaber (private communication).

[28] Hill, Salant, and Widgoff, Phys. Rev. **98**, 247(A) (1955).

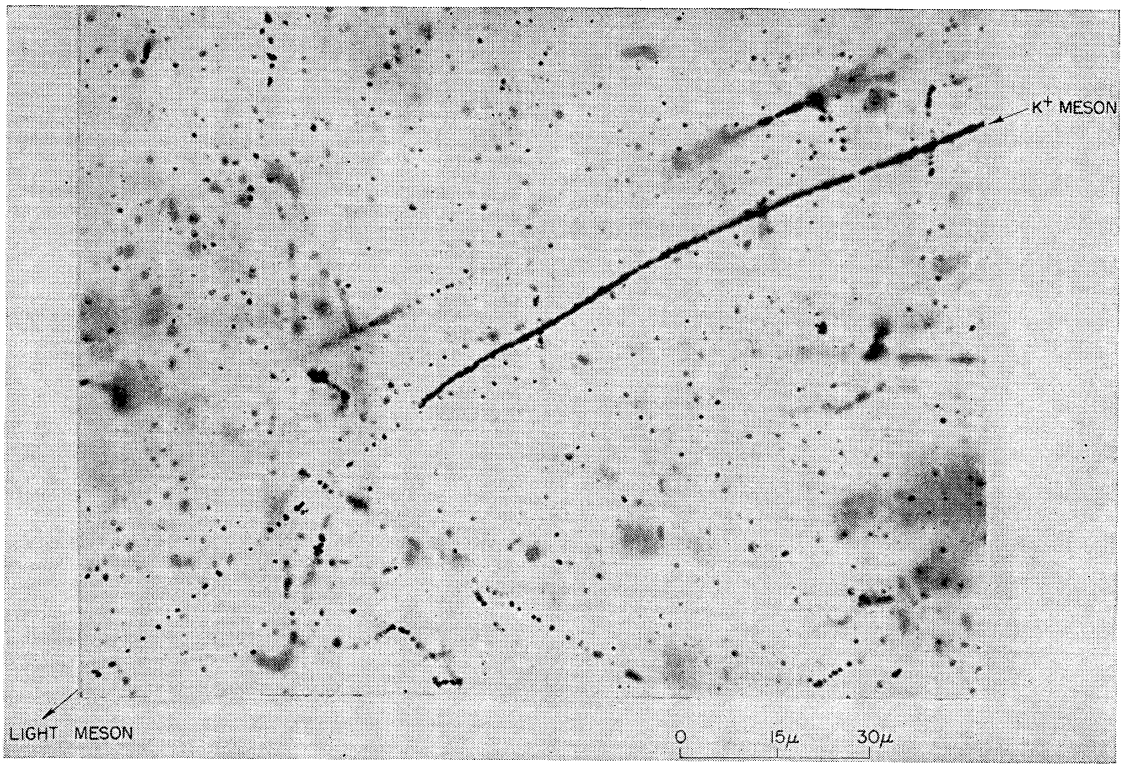

FIG. 4. Decay of K^+ meson. A K^+ meson coming from the right is shown stopping and decaying into an outgoing light meson.

histograms for a particular emulsion, *LT5a7*, are shown in Fig. 5. Figure 5(a) shows a histogram of the grain counts of electrons from μ-e decays; Fig. 5(b) shows a histogram of blob counts of the same electrons. The distribution of the blob counts can be seen to be narrower, probably because blob counting is less liable to subjective errors. It thus appears to be advantageous to use blob rather than grain counting for tracks of near-minimum ionization.

The calibration counting was done on long tracks which showed relatively little scattering, and the electrons used probably all had energies of about 10 Mev or more. The blob count thus obtained has been taken to be the plateau blob count, b_{plat}.

The scattering and blob density measurements on the decay-product track of *K*10 were made over the first 4.9 cm of its range. The last 0.35 cm of the track in the emulsion approached the edge of the plate and was not measured because of the possibility of distortion. The primary cell length used in the scattering measurements was 100μ, and the mean scattering angle, $\bar{\alpha}_{100}=0.171°\pm0.006°$, was obtained from the 100μ and 200μ values of the mean second difference by using the noise elimination technique of Menon, O'Ceallaigh, and Rochat.[18] If one uses the value[29] 24.3 (Mev/c)-deg for the scattering constant, as is consistent with the measured ratio, $b/b_{\text{plat}}=1.18$, of average blob density to plateau blob density, one obtains for the average $p\beta$ of the track a value of (139±8) Mev/c.

TABLE VII. Details of τ-meson decays.

τ meson	π mesons (charge where known)	Pion energies (Mev)	Lengths pion tracks (mm)	Relative angles (degrees)	Q value (Mev)
$\tau1$	$\pi1^+$	15.4	4.9	61.3	75.6±1.0
	$\pi2$	16.8	4.6	150.0	
	$\pi3$	43.4	8.1		
$\tau2$	$\pi1$	34	1.95	126.2	79±12
	$\pi2$	24	0.47	131.3	
	$\pi3$	21	0.27		

It was apparent that the scattering angle increased with distance from the origin of the track. For the purpose of analysis, the track was therefore divided into six segments and the mean scattering angle, $\bar{\alpha}_{100}$, computed for each segment. The segment with the largest scattering was ~3.5 mm long, each of the other segments ~9 mm. The values so obtained are given in Table VIII.

The blob density was measured along the whole length of the track and showed a significant increase with distance from the origin. The measured blob densities for the six sections of the track under con-

[29] Bristol curves, based on work of L. Voyvodic and E. Pickup (private communication).

sideration are also shown in Table VIII. The total numbers of blobs counted in each section were of the order of 3000, so that the statistical mean deviations in blob densities are of the order ± 0.6 blobs per 100μ. The tracks of fast electrons in close proximity to the K-secondary track showed slight local variations (~ 3 percent) in plateau blob density. The values of b^* are the blob densities corrected for these local variations. The ratios of b^* to b_{plat} are given in the final column of Table VIII.

Each of the secondary outgoing tracks of $K2$, $K3$, and $K7$ mesons was scattered in three adjacent emulsions. In order to indicate the possible degree of accuracy of the scattering measurements, the separate mean second scattering differences are shown in Table IX. It is seen from these values that, with the possible exception of the case $K7$, the constancy of both $\bar{D}_{100\mu}$ and $\bar{D}_{200\mu}$, as well as the ratio $\bar{D}_{200\mu}/\bar{D}_{100\mu}$, is not very good. No correction for distortion was made because the numbers of independent second differences of both positive and negative signs were always approximately

TABLE VIII. Summary of scattering and blob density measurements for the secondary track of $K10$.

Distance of midpoint of track segment from origin (mm)	$\bar{\alpha}_{100}$ (degrees)	$p\beta$ (Mev/c)	b^* (blobs per 100μ)	b^*/b_{plat} ($b_{\text{plat}}=29.5\pm0.3$)
4.35	0.148 ± 0.022	163 ± 24	33.0 ± 0.6	1.12 ± 0.03
13.05	0.143 ± 0.020	170 ± 23	34.2 ± 0.6	1.16 ± 0.03
21.75	0.151 ± 0.020	161 ± 21	34.8 ± 0.6	1.18 ± 0.03
30.45	0.181 ± 0.025	134 ± 19	35.3 ± 0.6	1.20 ± 0.03
39.70	0.213 ± 0.028	114 ± 15	37.0 ± 0.6	1.25 ± 0.03
46.75	0.240 ± 0.045	101 ± 19	37.3 ± 0.7	1.26 ± 0.04
Whole track	0.174 ± 0.010	139 ± 8	34.8 ± 0.3	1.18 ± 0.01

the same. The values of $\bar{\alpha}_{100}$ were obtained by using the noise elimination procedure.

Blob counting on the outgoing tracks showed no significant variation from one emulsion to another. The ratios b^*/b_{plat} are given in the final column of Table IX. The errors quoted are the standard deviations based on the numbers of grains counted.

The values of b^*/b_{plat}, from Tables VIII and IX are plotted as a function of $p\beta$ in Fig. 6.

For various reasons, enough pion tracks for good blob count-$p\beta$ calibration in the relevant emulsion strips have not yet been obtained. While the search for the appropriate tracks is still going on, it was regarded as instructive to compare the measured values of the K secondaries with pion ionization-$p\beta$ curves obtained in other laboratories. These curves are drawn solid in Fig. 6, from the values given by (a) Daniel *et al.*,[30] (b) the group at the University of Padua,[31] and (c) Fleming and Lord.[32] The muon curves in Fig. 6 are

[30] Daniel, Davies, Mulvey, and Perkins, Phil. Mag. **43**, 753 (1952).
[31] Padua group (private communication by G. T. Zorn).
[32] J. R. Fleming and J. J. Lord, Phys. Rev. **92**, 511 (1953).

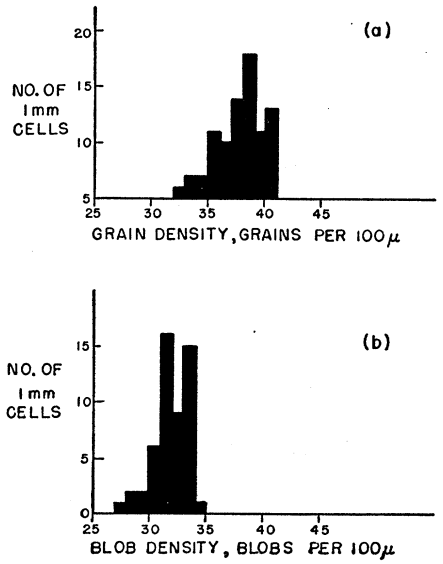

FIG. 5. Histograms of blob and grain densities. Figure 5(a) shows a histogram of grain counts on high energy electrons from μ-e decays. Figure 5(b) shows a similar histogram of blob counts on the same electrons as were used in obtaining Fig. 5(a).

derived in the usual way from the pion curves. In cases (a) and (b), the plateau blob densities were obtained from blob counts of pair electrons of energy >10 Mev and from primaries of high energy stars. For (a), the value is ~ 19 per 100μ, for (b) 22 per 100μ. The plateau blob density for (c), obtained from μ-decay electrons, was 30 per 100μ. Values of $p\beta$ were determined, in (a) and (b) by scattering measurements, in (c) by the more precise magnetic measurement of momentum of selected pion beams.

The secondaries of $K3$ and $K7$ are consistent with either the π or μ calibration curves.

In all three calibrations, the $K2$ secondary agrees with the μ but not with the π curve. It cannot be excluded, however, that any of the secondaries $K2$, $K3$, or $K7$ is an electron.

TABLE IX. Scattering and blob density determinations for secondary tracks of $K2$, $K3$, and $K7$ mesons.

K particle	Length scattered (mm) (emulsion number)	$\bar{D}_{100\mu}$ (μ)	$\bar{D}_{200\mu}$ (μ)	$\bar{\alpha}_{100}$ (degrees)	$p\beta$ (Mev/c)	b^*/b_{plat}
$K2$	2.5 (6)	0.0340	0.0980	0.182	134 ± 18	1.02 ± 0.03
	4.1 (7)	0.0331	0.1025			
	1.6 (8)	0.0202	0.0395			
$K3$	2.4 (8)	0.0211	0.0639	0.131	186 ± 30	0.99 ± 0.04
	2.1 (9)	0.0201	0.0830			
	1.4 (10)	0.0239	0.0354			
$K7$	4.1 (22)	0.0281	0.0739	0.127	192 ± 22	1.02 ± 0.03
	4.2 (23)	0.0251	0.0583			
	3.3 (24)	0.0243	0.0587			

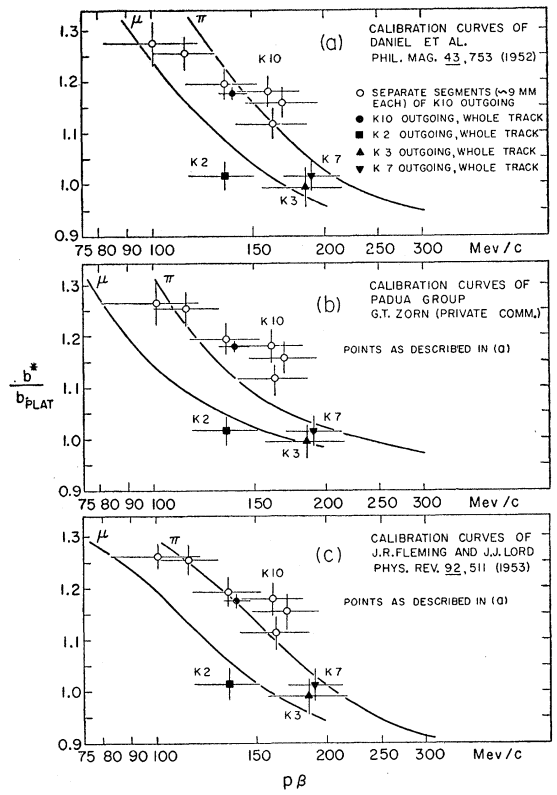

FIG. 6. Plots of blob densities *vs* $p\beta$-values for the outgoing light mesons of K^+ mesons: $K2$, $K3$, $K7$, and $K10$. Figures 6(a), 6(b), and 6(c) show these data plotted relative to the π- and μ-meson curves of Daniel *et al.*, the Padua Group, and Fleming and Lord, respectively.

In all three calibrations, the $K10$ secondary for $p\beta \geq 134$ is consistent with the π but not with the μ curve. For $p\beta = 114$, $K10$ is consistent with the π curves but not with the μ curves of (b) and (c), while it could be just as well associated with either curve of calibration (a). The less precise point at $p\beta = 101$ could lie either on the π or μ curves of (b) and (c), and better on the μ than on the π curve of (a).

The fit of the higher $p\beta$ points to all π calibration curves and failure of those points to fit the μ curves are evidence that the $K10$ secondary is a pion. The discrepancy between the low $p\beta$ points and the Daniel π curve arises because the $K10$ points lie on a flatter curve. Since the plateau density in the Brookhaven plates is 29.5 and in the Daniels plates only 19, this greater flatness is not surprising in view of saturation effects. The Padua plates have plateau density 22, and curve (b) also is steeper than the $K10$ curve. The plateau density of the Fleming-Lord plates is the same as for the Brookhaven plates (and both were determined in the same way, from μ-decay electrons) and the slopes of the $K10$ and (c) curves are quite consistent with each other.

The point representing the average $p\beta$, (139±8) Mev/c, and average blob density of the entire $K10$ track is consistent with the π curves but not with the μ curves of all three calibrations. The average $p\beta$ of $K2$ is (134±18) Mev/c. Hence it can be stated that, at approximately the same $p\beta$, the blob density of $K10$ is 20 percent higher than the blob density of $K2$. This supports the evidence for identifying the $K10$ secondary as a pion.

If one accepts this evidence that the $K10$ secondary is a pion, one finds, from the $p\beta$ measurements and the known rate of energy loss in emulsion, its $p\beta$, momentum and kinetic energy at emission as 165±7 Mev/c, 198±7 Mev/c and 102±6 Mev, respectively.

That positive K mesons might decay into two light mesons, a positive pion and a neutral secondary, was first suggested by Menon and O'Ceallaigh,[33] who observed five cases in which the $p\beta$ of the decay particle was approximately constant and lay between 162 and 187 Mev/c. A similar case was later observed by Bonetti *et al.*,[34] who determined the $p\beta$ of the decay particle as 200±33 Mev/c.

It was mentioned in the preliminary report[28] that, if the $K10$ decay is represented by

$$K^+ \rightarrow \pi^+ + \pi^0 + Q,$$

then (with masses[16,35] $m_{\pi^+} = 273.4 m_e$ and $m_{\pi^0} = 263.7 m_e$) $Q = 207 \pm 9$ Mev and the mass of the $K10$ primary is $(945 \pm 20) m_e$.

The primary track $K10$ was not long enough to make possible a precise direct measurement of its mass; the values obtained by constant sagitta scattering methods and given in Table VI are not inconsistent with the value deduced from the assumed decay.

Thus the event $K10$, the recent Princeton cloud-chamber observation,[36] and two recent K^+ decays in emulsions[37] are very similar. The K-meson mass and the Q agree closely[9] with the mass and Q of the θ^0, which decays into two charged pions.

Since it is not certain that the $K10$ primary came directly from the target, nothing significant can be said about its lifetime.

ACKNOWLEDGMENTS

We are indebted more than we can say to Mrs. M. Hall and the other scanners, Mrs. M. Bracker, Mrs. B. Cozine, and Mrs. A. Lea. We take pleasure in thanking Mrs. M. Carter, Mr. J. Smith, and Mr. J. Quinn for

[33] M. G. K. Menon and C. O'Ceallaigh, Proc. Roy. Soc. (London) **A221**, 292 (1953).
[34] Bonetti, LeviSetti, Panetti, and Tomasini, Proc. Roy. Soc. (London) **A221**, 318 (1953).
[35] W. Chinowsky and J. Steinberger, Phys. Rev. **93**, 586 (1954).
[36] Hodson, Ballam, Arnold, Harris, Rau, Reynolds, and Treiman, Phys. Rev. **96**, 1089 (1954).
[37] Baldo, Belliboni, Sechi, and Zorn, Nuovo cimento **12**, Suppl. 2 (Padua Conference), 220 (1954).

preparing and processing the emulsions, Dr. R. Sternheimer for informative discussions of the theoretical aspects of K-particle production, and Dr. M. Goldhaber, Dr. J. Hornbostel, and Dr. G. Zorn for helpful criticisms and suggestions. And of course the exposures would not have been possible without the willing and able services of the Cosmotron Staff. Dr. Marcel Schein of the University of Chicago very generously sent us a precision stage which was used for the scattering measurements.

PHYSICAL REVIEW VOLUME 99, NUMBER 1 JULY 1, 1955

Hydromagnetic Waves and the Acceleration of Cosmic Rays*

EUGENE N. PARKER
Department of Physics, University of Utah, Salt Lake City, Utah
(Received January 27, 1955; revised manuscript received March 15, 1955)

The large amounts of energy necessary for the acceleration of cosmic rays throughout the galaxy introduces a serious transport problem. The hydrodynamic and hydromagnetic equations are investigated from the viewpoint of energy propagation. It is shown that, with the galactic model of Fermi and Chandrasekhar, the observed motions of the interstellar gas reduce to hydromagnetic waves, which are, as it turns out, the most effective means of energy transport. A consideration of the interaction of charged particles with hydromagnetic waves shows that it is the fluid velocity, and not the wave velocity, that is responsible for the acceleration of cosmic rays by Fermi's mechanism.

We calculate the the dissipation of hydromagnetic waves in the interstellar medium, and the variation of amplitude and wavelength of such waves with changes in density and large-scale field intensity. It is then shown that the galaxy is no more than one percent efficient in the acceleration of cosmic rays because of the tremendous viscous losses in the interstellar medium, and that there is no hydromagnetic mechanism that can convert the observed large-scale low-velocity fluctuations in the interstellar medium to the required small-scale high-velocity motions.

MORRISON, Olbert, and Rossi[1] have discussed the necessary conditions for accelerating, by Fermi's mechanism,[2,3] the cosmic-ray particles observed at the earth. The energy they require for the acceleration comes directly from the irregular motions of the gas clouds in the spiral arms of the galaxy. So much energy is needed to accelerate the cosmic-ray particles that the clouds would lose their irregular motions in a period of time of the order of only 10^6 years. There seem to be only two sources of energy of sufficient magnitude to supply the clouds for significant periods of time: One is the gravitational energy of the galaxy as a whole; and the other is the nuclear energy continually liberated in the interior of stars. Though it is not clear as to how the gravitational energy of the galaxy can excite the small scale cloud motions, Oort[4] and Spitzer[5] have recently proposed a mechanism whereby the O and B stars can transfer large amounts of energy to the motions of the gas clouds: The O and B stars, with their enormous surface temperatures, ionize and explode the gas clouds near whose centers they are formed.

The average life of a cosmic-ray particle based on collision length is of the order of 4×10^7 years. Morrison *et al.* find, however, that before the particle escapes from the galaxy a life of no more than 4×10^6 years can be tolerated in view of the observed mass spectrum. Since the energy density of cosmic rays is about the same as starlight, *viz.* 5×10^{-13} erg/cm^3,[6] they require 3×10^{-27} erg/cm^3/sec for the acceleration of cosmic rays, instead of only 3×10^{-28} erg/cm^3/sec based on the lifetime of 4×10^7 years.

Now, whatever the source of the energy maintaining the irregular motions of the gas clouds, whether it be Oort's mechanism alone or this mechanism in conjunction with other sources, there must be some means for propagating the irregular motion from the relatively localized sources of supply, *viz.*, the O and B complexes. The bodily transport of kinetic energy by the moving clouds themselves is very inefficient because the transfer to other clouds is through the inelastic collisions between clouds. We are led to consider the possibility of more efficient transport processes, and toward this end we shall now decompose the equations of hydrodynamics and hydromagnetics into components according to the manner in which they propagate.

I. HYDRODYNAMICS

It is well known that for suitable boundary conditions there exist functions $\mathbf{A}(\mathbf{r})$ and $\varphi(\mathbf{r})$, where $\mathbf{r}$ represents the position vector, such that any analytic vector function $\mathbf{v}(\mathbf{r})$ may be expressed[7] as

$$\mathbf{v}(\mathbf{r})=\nabla\times\mathbf{A}(\mathbf{r})-\nabla\varphi(\mathbf{r}),\quad \nabla\cdot\mathbf{A}(\mathbf{r})=0. \tag{1}$$

Taking the curl and the divergence of this expression,

* This work was supported by the Office of Naval Research.
[1] Morrison, Olbert, and Rossi, Phys. Rev. **94**, 440 (1954).
[2] E. Fermi, Phys. Rev. **75**, 1169 (1949).
[3] E. Fermi, Astrophys. J. **119**, 1 (1954).
[4] J. H. Oort, Bull. Astron. Soc. Netherlands **12**, 177 (1954).
[5] J. H. Oort and L. Spitzer, Jr., Astrophys. J. **121**, 6 (1955).
[6] T. Dunham, Jr., Am. Phil. Soc. **81**, 277 (1939).
[7] C. F. Sommerfeld, *Mechanics of Deformable Bodies* (Academic Press, Inc., New York, 1950), p. 147.

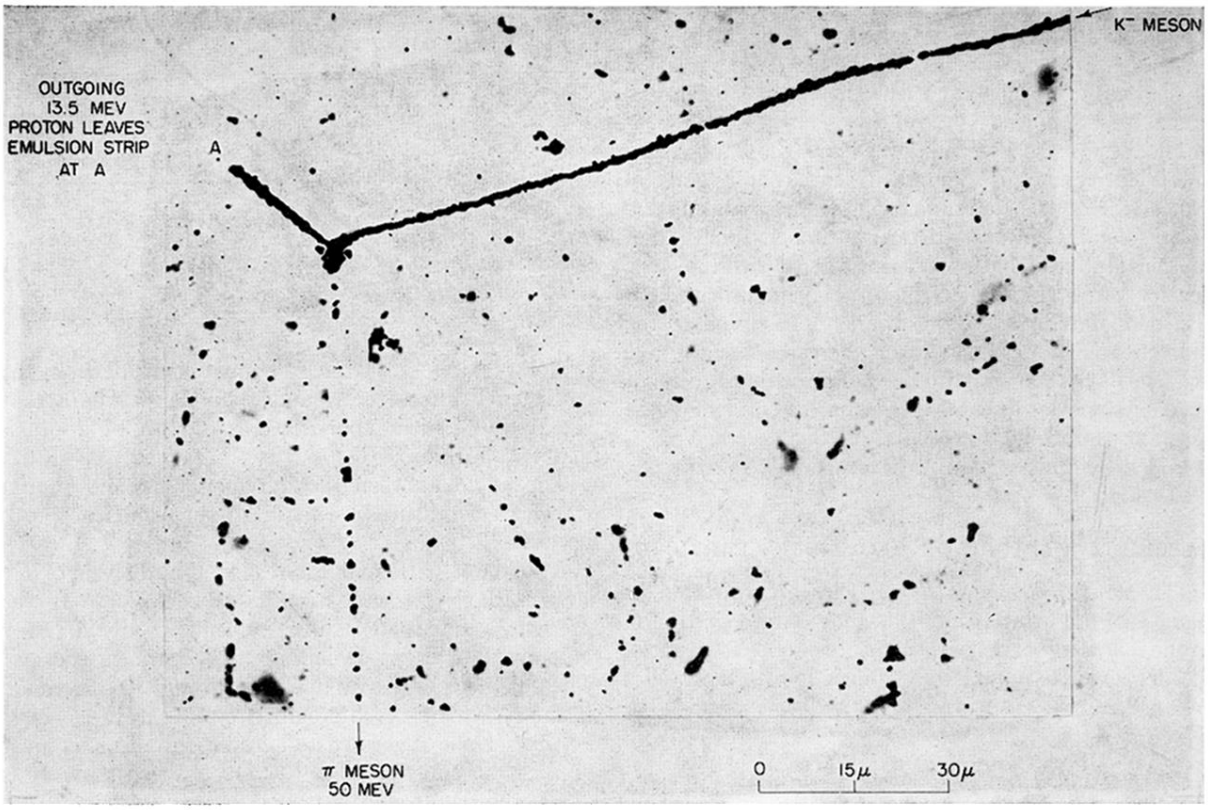

FIG. 2. Star produced by capture of K^- meson. A K^- meson coming from the right is shown stopping and producing a two-prong star of a π meson and a proton.

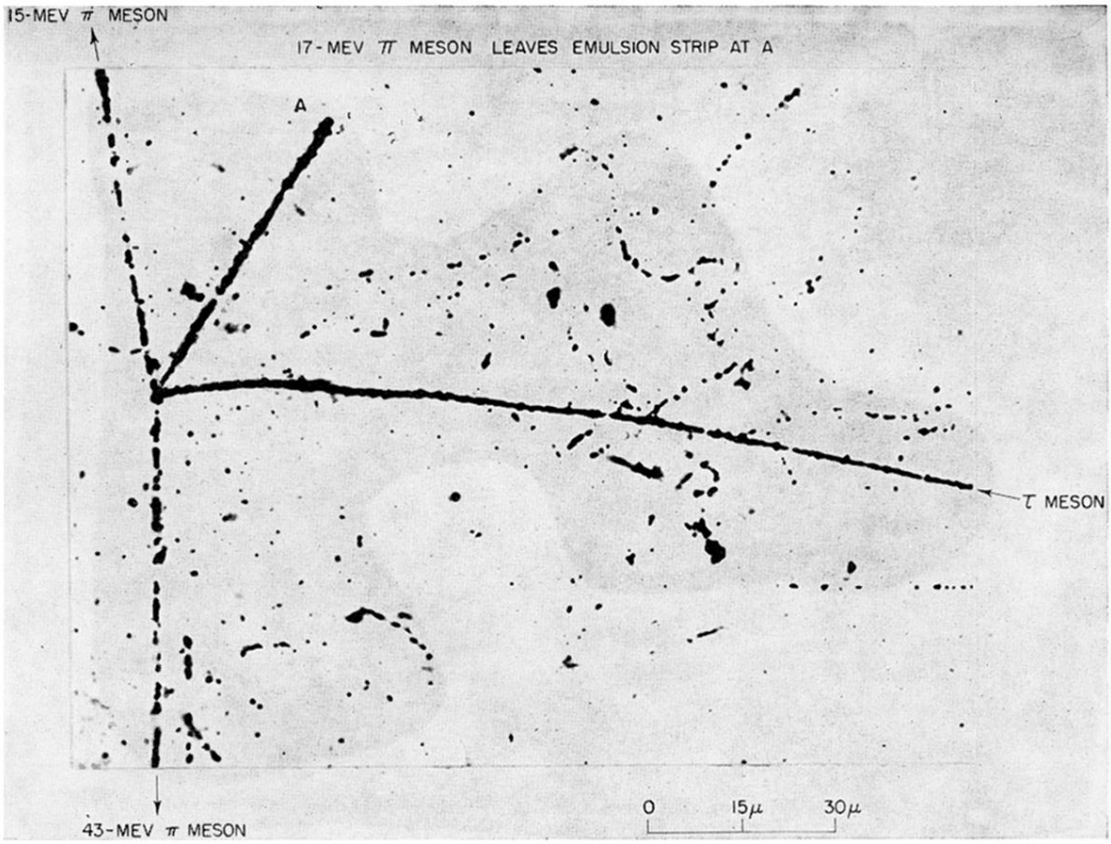

FIG. 3. Decay of τ meson. A τ meson coming from the right is shown decaying at rest into three coplanar charged π mesons.

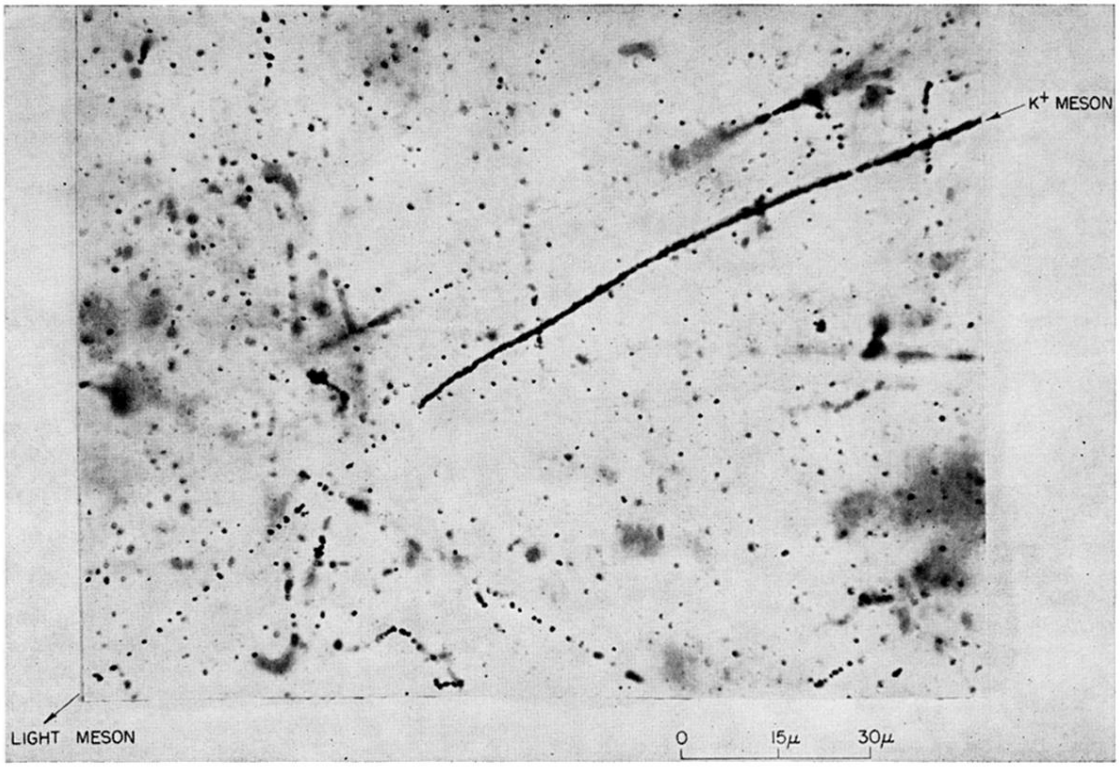

FIG. 4. Decay of K^+ meson. A K^+ meson coming from the right is shown stopping and decaying into an outgoing light meson.